J Mater Sci (2010) 45:4470–4479
DOI 10.1007/s10853-010-4531-3

Effects of CTAB on porous silica templated by chitosan

Lixia Wang · Jiangjiexing Wu · Xian Wang · Qin Cheng · Lin Zheng · Jinli Zhang · Wei Li

Received: 18 January 2010 / Accepted: 13 April 2010 / Published online: 30 April 2010

Abstract Understanding the interaction between chitosan and surfactant cetyltrimethylammonium bromide (CTAB) is fundamental to prepare nanoparticles for drug delivery but also to synthesize porous functionalized materials. In this work, we first studied the self-aggregation property of chitosan and found that the microporous structure of chitosan-templated silica was dependent on the chitosan concentration and the deacetylation degree of chitosan. The interactions between chitosan and CTAB were studied by reflection–absorption infrared spectra, which illustrate that the molecular orientations of chitosan are greatly affected by adding CTAB especially at lower pH. Through measurements of the critical micelle concentration values of CTAB and characterizations of porous structures, it is indicated that micro–meso silica can be synthesized with the chitosan–CTAB hybrid, and both surface area and pore volume as well as the meso-periodity of silica can be modulated by adding CTAB in the sol–gel synthesis process at proper pH value.

Introduction

Chitosan, poly-β-(1-4)-2-amino-2-deoxy-D-glucose, is produced from partial *N*-deacetylation of chitin, and has been recently studied as the promising nonviral carrier candidates for drug delivery, owing to the strong electrostatic interactions between amino groups of chitosan and proteins or genes [1, 2]. In order to modulate the property of chitosan nanoparticles, surfactants have been investigated as the interfacial modifiers during the fabrication. For example, Thongngam and McClements [3, 4] reported that the interaction between chitosan and anionic surfactant sodium dodecyl sulfate (SDS) was dominantly affected by the electrostatic interactions. Li et al. [5] concluded that carboxymethylchitosan, a derivative of chitosan, can form network structures with cetyltrimethylammonium bromide (CTAB). Bao et al. [6] reported that CTAB can affect the size of nanoparticles prepared by the crosslinking reaction between chitosan and pentasodium triphosphate. These results suggest that ionic surfactants play an important role in controlling the aggregation property of chitosan. However, no report has been found on the interaction between the positively charged CTAB and chitosan so far, which is fundamental to prepare nanoparticles for drug delivery.

On the other hand, porous materials with hierarchical structure including micro–meso, meso–meso, and meso–macro offer attractive properties for a variety of applications such as catalysis reaction [7, 8], adsorption separation [9, 10], and drug delivery [11, 12], etc. [13–15]. A number of polymers and surfactants have been studied as co-templates to adjust the porous structures in different length scales of materials [16–20]. Pedroni et al. [21] has synthesized mesoporous–macroporous siliceous materials via hydrothermal hydrolysis using the template of chitosan with the deacetylation degree (DD) of 90%. Chitosan was reported to be capable of aggregating into micelle-like agglomerates, dependent on its DD [22]. Thus, it is important to investigate the self-aggregation property of chitosan with different DD as well as its effect on modulating the porous structures.

L. Wang · J. Wu · W. Li (✉)
Key Laboratory for Green Chemical Technology MOE, Department of Chemical Engineering, School of Chemical Engineering & Technology, Tianjin University, Tianjin 300072, People's Republic of China
e-mail: liwei@tju.edu.cn

X. Wang · Q. Cheng · L. Zheng · J. Zhang
Key Laboratory of Systems Bioengineering MOE, School of Chemical Engineering & Technology, Tianjin University, Tianjin 300072, People's Republic of China

In this article, microporous silica were first synthesized using the template of chitosan, based on investigating the self-aggregation property of chitosan as a function of the DD using fluorescence probe technique. Interactions between CTAB and chitosan were studied using reflection–absorption infrared spectroscopy (RAIR), and the critical micelle concentration (CMC) of CTAB were measured at different pH and temperature, in order to disclose the effect of CTAB on modulating pore structures of chitosan-templated silica. It is illuminated that pH-dependent interactions between chitosan and CTAB can affect the molecular orientation of the chitosan–CTAB hybrid, which plays an important role in adjusting the meso-periodity of the micro–meso porous silica.

Materials and methods

Chemicals

Chitosan, with the weight average molecular weight of 1.6×10^5 and the DD of 88%, was purchased from Jinan Ocean Biotechnology Company of China. In order to obtain different chitosan samples with the desired DD ranged from 54 to 88%, the raw material chitosan was solved in an acetic acid solution and then mixed with an acetic anhydride–methanol solution to react at 30 °C for 6 h, adjusting the molar ratio of acetic anhydride to the glucosamine group of chitosan within 0.2–0.8 [23].

Cetyltrimethylammonium bromide (CTAB, 98%) was purchased from Shanghai Shi Yi Chemicals Co. (China) and was used as-received. Pyrene (99%, Sigma) was used as the fluorescent probe.

Templated synthesis of porous silica

Microporous silica samples were synthesized by using the chitosan template via the sol–gel technique. A tetraethoxysiliane (TEOS) ethanol solution was quantitatively dropped into a chitosan aqueous solution containing dilute acetic acid (4 wt%) at 30 °C with stirring for 6 h. The obtained solution was desiccated at room temperature to obtain a gel, followed by the calcination at 550 °C for 2 h. The chitosan/TEOS molar ratio of the samples was calculated from the molecular weight of the monomer unit of chitosan (160.1), and denoted as Cs:TEOS.

Micro–meso porous silica samples were synthesized by using the chitosan–CTAB hybrid via the sol–gel method and the hydrothermal method, respectively. In the sol–gel procedure, a mixed solution was first prepared by adding the CTAB ethanol solution into the acidic aqueous solution of chitosan, then the TEOS ethanol solution was dropped quantitatively into the above chitosan–CTAB mixing solution at 30 °C to react 6 h, followed by gelation and calcination at 550 °C for 2 h. The chitosan/CTAB molar ratio of the silica sample was calculated from the molecular weight of the monomer unit of chitosan (160.1), and denoted as Cs:CTAB.

While via the hydrothermal method, the mixture obtained by dropping the TEOS ethanol solution into the chitosan–CTAB solution was maintained in an autoclave at 80 °C for 12 h; then the obtained product was dried and calcined at 550 °C for 2 h.

Characterization

Steady-state fluorescence measurements were performed with Cary Eclipse (Varian Ltd.) using pyrene as the probe [24] to study the critical aggregation concentration (CAC) of chitosan with different DD in acidic aqueous solution, or to determine the CMC of CTAB under different pH and temperatures. Pyrene probe was excited at 337 nm and the emission spectra were recorded in the range of 350–500 nm.

N_2 adsorption–desorption isotherms were measured via a micromeritics ASAP 2020 analyzer. The specific surface area (S_{BET}) was estimated using adsorption data in the relative pressure from 0.04 to 0.2 and the total pore volume (V_{total}) was determined from the amount adsorbed at a relative pressure of 0.99. The size of the micropore was determined by using the Horvath–Kawazoe (HK) method with slit pore geometry. Micro–mesopore size distribution was calculated by density functional theory (DFT) [25–27] from the N_2 adsorption isotherm. Microporosity is calculated using the ratio of S_{micro}/S_{total}.

AFM images were collected on an AJ-III atomic force microscopy (Shanghai AJ-Nano Company, China) by the tapping mode. The size and morphology of aggregates were analyzed by the standard software accompanied the AFM. Samples for AFM imaging were prepared by depositing about 10 μL chitosan solution on freshly cleaved mica surface and dried under room temperature.

Reflection–absorption infrared spectroscopy is useful to characterize the molecular structure and orientation in the thin films of polymers. The film samples of chitosan or the chitosan–CTAB mixture were spin-coated onto the clean plane (110) of the silicon wafer substrate, with the size of 1 cm × 1 cm × 520 μm. A Nicolet iS10 FT spectrometer equipped with the Model 500° variable angle specular reflectance accessory and the MCT detector was used to obtain the spectra. The RAIR measurement was obtained by averaging 32 scans at an incidence angle of 45° and a resolution of 4 cm^{-1}. The spectrum of the clean plane (110) of silicon wafer was subtracted from all RAIR spectra of film-covered substrates.

TEM images of samples were obtained using a JEM-100X transmission electron microscope operating at 100 kV.

Samples for TEM measurements were prepared by dropping appropriate amount of solutions onto the carbon film covered on a Cu grid, and dried at room temperature.

X-ray diffraction (XRD) patterns were measured on a D/MAX-2500 (Japan) power X-ray diffractometer system (40 kV, 100 mA) with Cu$K\alpha$ radiation. The diffractograms were recorded over a 2θ range of 0.6° to 50°.

Results and discussion

Self-aggregation of chitosan and its templated microporous silica

Critical aggregation concentration of chitosan with the DD ranging from 54 to 88% was studied by using fluorescence measurements at 30 °C taking pyrene as the probe. Figure 1a shows the representative fluorescence spectra of pyrene in the acidic solution of chitosan, which display five distinct vibration peaks. The intensity ratio of the first and the third vibration band defined as "hydrophobic index" is proved to be useful in the study of the aggregation properties. Plots of peak intensity ratio I_1/I_3 versus the concentration of chitosan can be obtained to determine the CAC value by the intersection point of the horizontal fitting curve and the sharply decreasing region (Fig. 1b, c). It is indicated that the CAC value decreases as increasing the DD of chitosan, i.e., the CAC is reduced from 6.2 to 1.5 g L^{-1} when the DD increases from 54 to 88% at 30 °C in 0.3 M acetic acid aqueous solution.

Microporous silica was synthesized via the sol–gel method under the template of chitosan with DD 88 or 59%. Figure 2 indicates the adsorption/desorption isotherms and the pore size distribution of chitosan-templated silica. It is illustrated that silica samples templated by chitosan (DD 59%) have characteristic of type I isotherms of micropores, while those templated by chitosan (DD 88%) exhibit type I and IV isotherms, illustrating the existence of both micropores and mesopores. Pore size distributions of the chitosan-templated silica are related with the concentration of chitosan template. In the case of using chitosan DD 59% as the template, the modal pore width is located respectively at 0.80, 1.0, and 1.2 nm at the low concentration of chitosan, and turns to be 0.59, 0.73, 1.3 nm and a broad band around 2.0 nm at the high concentration of chitosan. As for the template of chitosan DD 88% at the high concentration, the pore size distribution shows the micropores as alike as those templated by chitosan DD 59%, besides the appearance of a broader band around 3.0–9.0 nm. Similarly, the surface area and the pore volume of chitosan-templated silica are also augmented with increasing the concentration of chitosan, as listed by Table 1.

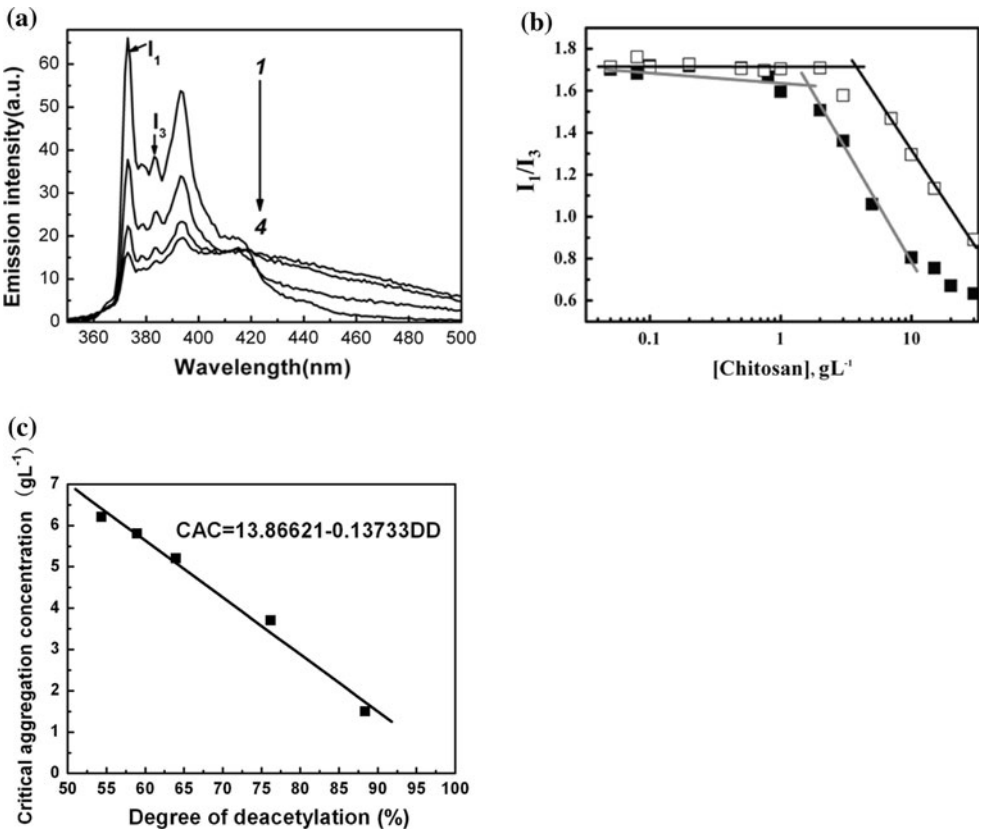

Fig. 1 **a** Fluorescence spectra of pyrene in acidic solutions of chitosan (DD 76%) at 30 °C under different concentrations of chitosan (1) 0.10 g L^{-1}, (2) 6.0 g L^{-1}, (3) 10 g L^{-1}, (4) 15 g L^{-1}. **b** Plots of I_1/I_3 ratio as a function of chitosan concentration, (■) DD 88%, (□) DD 76%. **c** Critical aggregation concentrations of chitosan with the deacetylation degree (DD) ranged from 54 to 88% at 30 °C

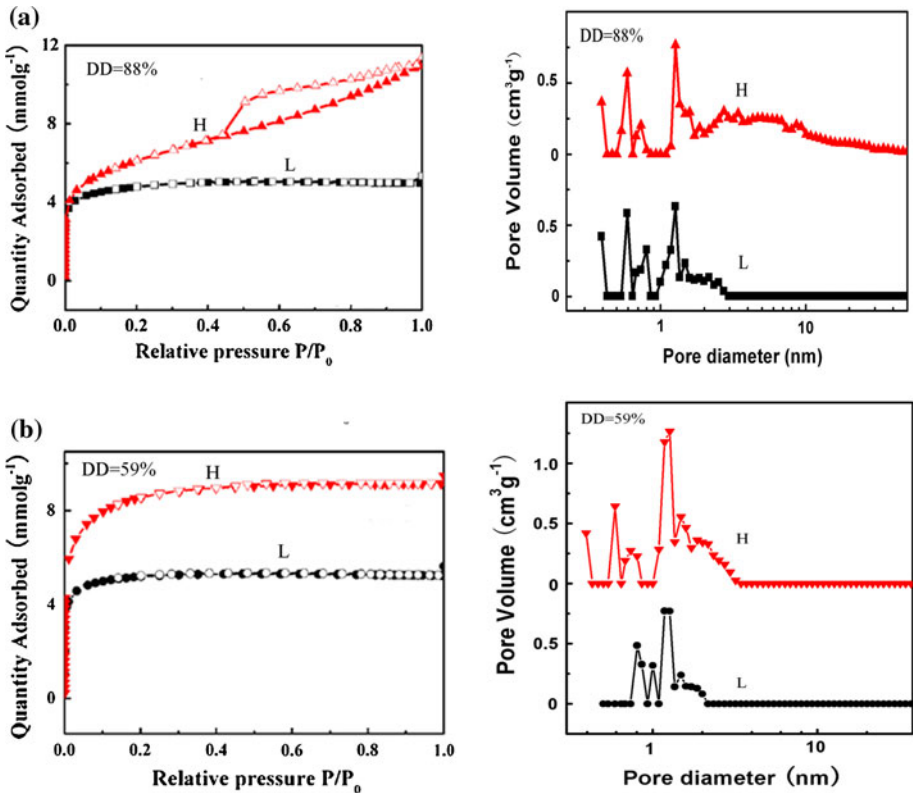

Fig. 2 N_2 adsorption–desorption isotherms of silica and the pore size distribution of microporous silica samples templated by chitosan with DD 88% (**a**) or DD 59% (**b**). L and H denote the molar ratio chitosan/TEOS of 1:25 and 4:25, respectively

Table 1 Structural parameters of microporous silica templated by chitosan

Chitosan (DD)	Cs/TEOS	S_{BET} (m^2 g^{-1})	V_{total} (cm^3 g^{-1})	Microporosity (%)
88%	1:25	367	0.185	97
	4:25	483	0.394	78
59%	1:25	395	0.195	100
	4:25	664	0.329	94

In addition, Table 1 indicates that the higher concentration of the chitosan template, the lower microporosity of silica is obtained. Especially silica samples synthesized using high-concentrated chitosan DD 88% exhibit a fraction of mesopores. The appearance of mesopores is attributed to the change of the size distribution of chitosan aggregates. Figure 3 shows AFM images of chitosan (DD 88%) aggregates at low and high concentration, respectively. It is obvious that the aggregates of chitosan at the high concentration have a number of large particles higher than 50 nm, whereas those at the low concentration are about 2–5 nm high.

Interactions between chitosan and CTAB

Reflection–absorption infrared spectroscopy is used to study the potential interactions between chitosan and CTAB. Figure 4 displays the RAIR spectra of the film comprising chitosan (DD 59% and DD 88%) or the chitosan–CTAB mixture at two different pH. As the DD value of chitosan increases from 59 to 88%, the intensities of the C=O stretching bands in the region of 1,720–1,730 cm^{-1} exhibit an obvious decrease while the intensities of the NH_2 stretching bands near 1,060 cm^{-1} increase greatly. For the chitosan–CTAB mixture with the chitosan/CTAB molar ratio of 1:1, the bands in the range of 2,845–2,910 cm^{-1} are assigned to the CH_3–(N^+) stretching vibration of CTAB. Owing to adopting CTAB, the C=O stretching bands of chitosan occur a blue-shift to the range of 1,630–1,650 cm^{-1}, and the intensities of the shifted bands become stronger at much acidic condition (pH 2.3). In addition, the NH_2 stretching bands of chitosan are red-shifted to the range of 1070–1080 cm^{-1}, especially for the chitosan (DD 59%) the red-shifted bands appear higher intensities. It is known that the formation of hydrogen bondings results in a blue-shift of the stretching vibration bands, and the band intensities in the RAIR spectra are dependent on the molecular orientation in the film [28, 29]. Therefore, it is suggested that upon mixing with CTAB more hydrogen bondings are formed around the C=O group

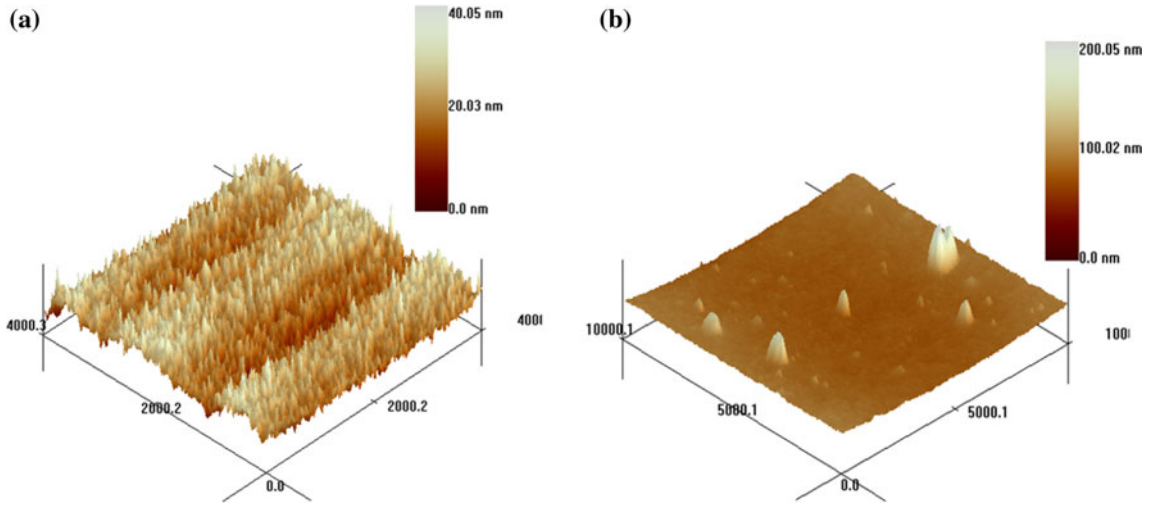

Fig. 3 AFM images of chitosan (DD 88%) aggregates at the concentration of 0.5 g/L (**a**) and 2.5 g/L (**b**), respectively

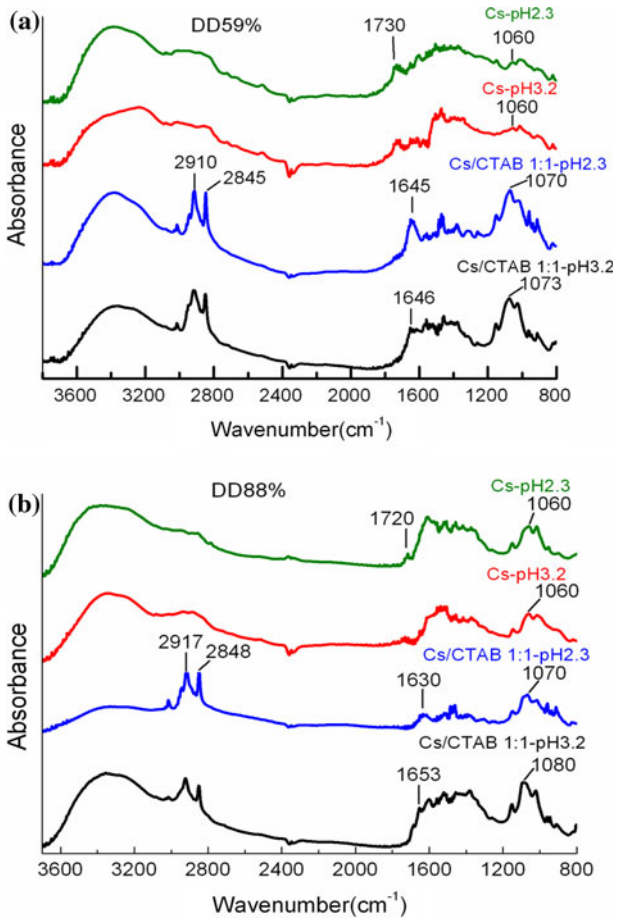

Fig. 4 RAIR spectra of chitosan and chitosan–CTAB hybrid with the chitosan/CTAB molar ratio of 1:1, **a** DD 59%, **b** DD 88%

of chitosan especially at lower pH, whereas fewer hydrogen bondings exist around the NH_2 group of chitosan, and the pH-dependent interactions can affect the molecular orientations of chitosan–CTAB hybrid.

Interactions between chitosan and CTAB are further confirmed by TEM images, as shown in Fig. 5. It is indicated that chitosan (DD 59%) at pH 2.3 forms spheric agglomerates with the radius around 10 nm, whereas the chitosan–CTAB hybrid assembles into orderly network structures. It is the influence of CTAB that modulates the molecular orientation of chitosan, which results in the transformation of chitosan aggregates from spheres into the network structures.

As far as the influence of pH on the self-assembly property of CTAB is considered, the CMC value of CTAB was measured by using fluorescent probe techniques. According to the plot of I_1/I_3 ratios versus CTAB concentrations where I_1/I_3 denoted the intensity ratio of the first (at 373 nm) and the third (at 384 nm) vibration bands in the fluorescence emission spectra (as shown by Fig. 6), the CMC value is determined as the CTAB concentration corresponding to the intersection between the extrapolating of the rapid decrease segments and the horizontal of the I_1/I_3 plot. It is worthwhile to mention that the ratio of I_1/I_3 decreases linearly along with the increase of CTAB concentration at 30 °C, while it appears two decreasing segments with one transition of the slope at 80 °C and pH lower than 2.7, suggesting the existence of non-uniformly shaped micelles in a relatively broad range of CTAB concentration, i.e., a slow transition process to form uniform micelles.

The CMC values of CTAB in the water–ethanol solvent (1:1, v/v) were also measured since the solvent is the mixture of water and ethanol during the synthesis of micro–mesoporous silica using the chitosan–CTAB hybrid. As listed by Table 2, it is indicated that the CMC of CTAB in water decreases with the pH value but increases with the temperature, i.e., the more acidic the aqueous solution, the smaller the CMC values; the higher the temperature,

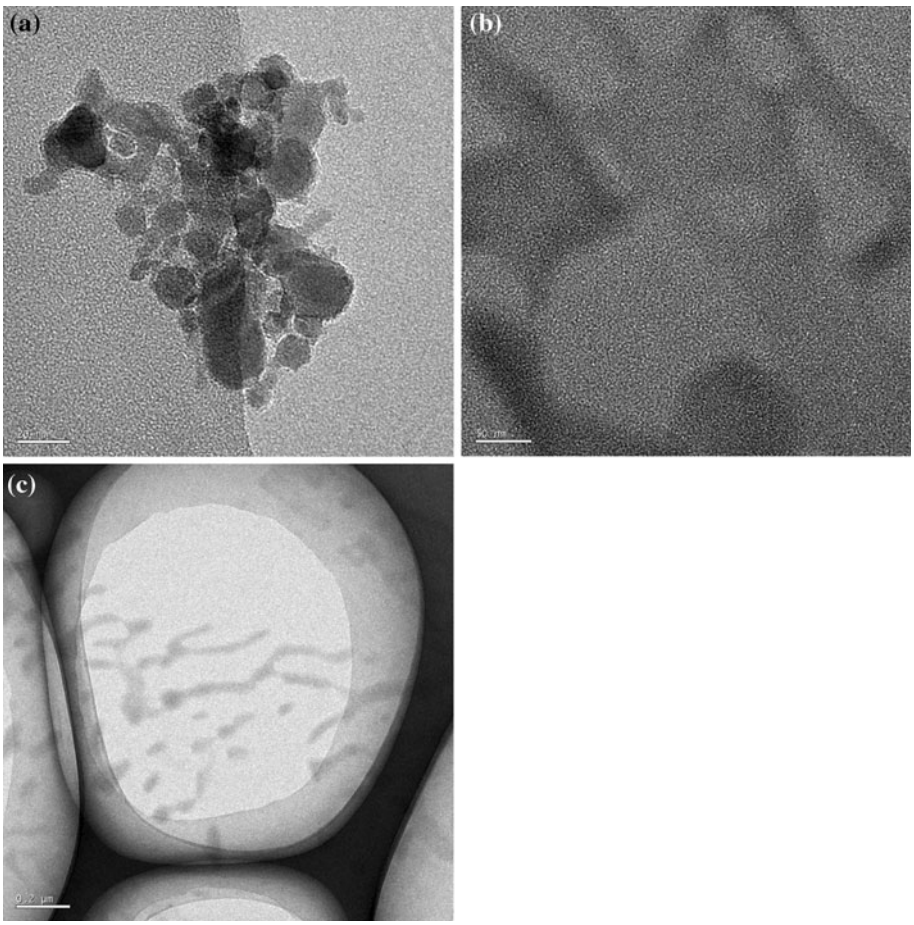

Fig. 5 TEM images of the aggregates of (**a**) chitosan (DD 59%) and (**b** and **c**) the chitosan–CTAB hybrid at pH 2.3

the larger the CMC values. However, in the water–ethanol solvent, the CMC of CTAB are obviously larger than those in water, and the influence of pH on the CMC is not the same as that in water—there exhibit the slow transition process of micelles even at 30 °C and pH lower than 2.1, whereas at 30 °C and pH higher than 2.7 the CMC of CTAB in the water–ethanol solvent is a definite value. When the temperature increases to 50 °C, the transition process of micelles is corresponding to a much broader region of CTAB concentration at pH ranged from 6.1 to 1.1.

Porous silica synthesized with the hybrid of chitosan–CTAB

Figure 7a, b show the adsorption/desorption isotherms and the pore size distribution of silica samples synthesized via the sol–gel technique with different ratio of chitosan (DD 59%)/CTAB under pH 3.2 and pH 2.3. The isotherms are typical of type IV curves, suggesting the coexistence of micro- and meso-pores. The pore size distribution of silica synthesized at pH 3.2 with the chitosan/CTAB ratio of 10:14 has the modal value at 1.1 nm and a broad band around 2.0 nm, while that at pH 2.3 has bimodal values around 1.3 and 2.8 nm.

On the other hand, silica samples synthesized via the hydrothermal method with the hybrid of chitosan (DD 59%) and CTAB show the adsorption/desorption isotherms of type IV curves with hysteresis loops, and the pore size distributes broadly around 1.2–1.7 and 2.0–6.3 nm (as shown by Fig. 7c).

As listed by Table 3, the surface area and the pore volume of the micro–mesoporous silica synthesized with the hybrid of chitosan–CTAB via the sol–gel method are significantly larger (925–1069 $m^2\ g^{-1}$; 0.486–0.625 $cm^3\ g^{-1}$) than those of chitosan-templated silica (395–664 $m^2\ g^{-1}$; 0.195–0.329 $cm^3\ g^{-1}$), while the microporosity of the silica (51–71%) is much lower than that of chitosan-templated silica (94–100%). Additionally the silica prepared using the hybrid of chitosan–CTAB via the hydrothermal method possesses lower surface areas and microporosity than those prepared via the sol–gel method.

According to the above measured CMC values of CTAB in the water–ethanol solvent, the definite CMC of CTAB at 30 °C and pH higher than 2.7 indicates the formation of uniform micelles, whereas the broad range of CMC of CTAB at 30 °C and lower pH or at higher temperature suggests a distribution of multiple shaped micelles. Uniformly shaped micelles are beneficial to prepare silica with

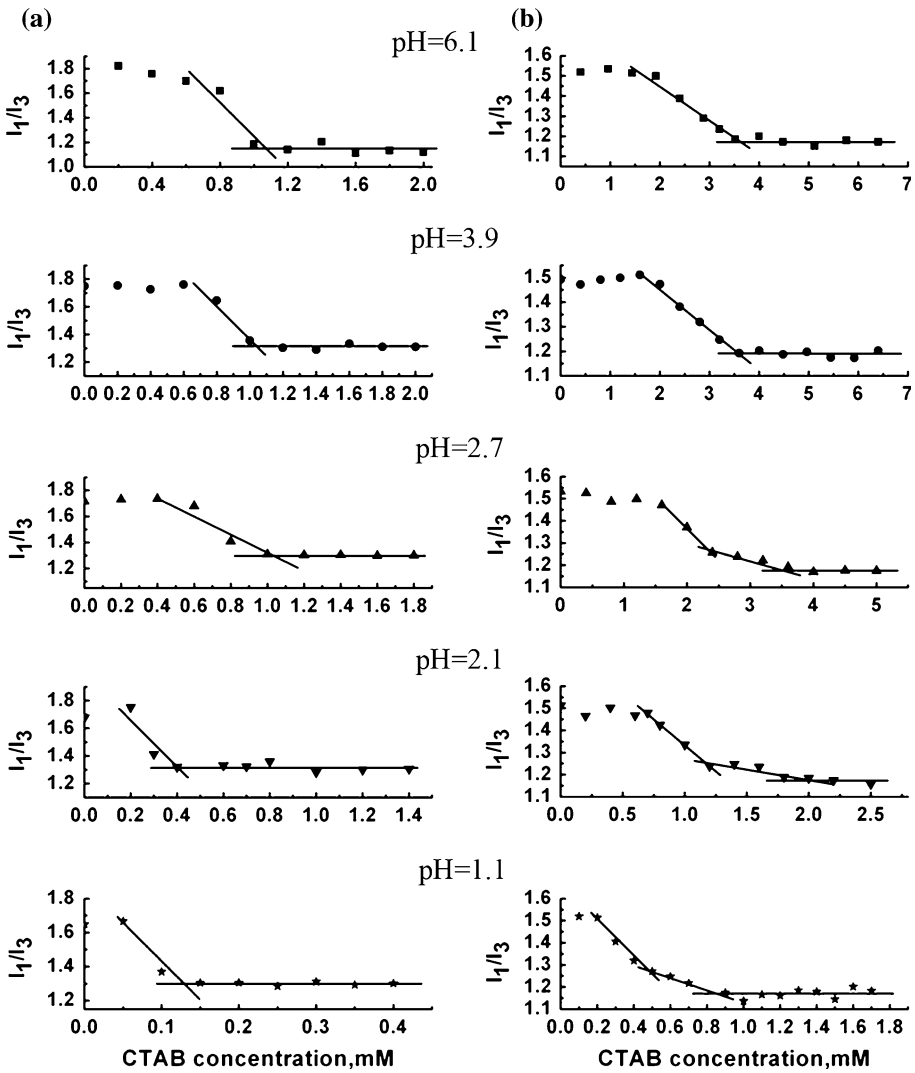

Fig. 6 Plots of the I_1/I_3 ratios versus CTAB concentrations at 30 °C (**a**, the *left panel*) or 80 °C (**b**, the *right panel*) in the aqueous solution under different pH values

Table 2 CMC values of CTAB at different pH and temperatures

Temperature (°C)	pH 6.1	pH 3.9	pH 2.7	pH 2.1	pH 1.1
CMC (mM, in the solvent of water)					
30	1.08	1.06	1.03	0.41	0.13
50	1.41	1.35	1.16	0.42	0.22
80	3.65	3.60	2.38–3.50	1.21–1.90	0.49–0.85
CMC (M, in the water–ethanol solvent 1:1 (v/v))					
30	0.055	–	0.087	0.054–0.102	0.069–0.130
50	0.056–0.172	–	0.049–0.165	0.060–0.161	0.075–0.167

the large surface area, therefore, the silica samples synthesized with the chitosan–CTAB hybrid via the sol–gel method at pH 3.2 have the largest surface area, followed by those synthesized via the sol–gel method at pH 2.3 and via the hydrothermal method successively (as listed by Table 3).

Figure 8 displays the small-angle XRD patterns of the micro–mesoporous silica samples synthesized with the hybrid of chitosan–CTAB. It is clear that silica samples synthesized via the sol–gel method at pH 2.3 exhibit the diffraction peaks around 2.0°, indicating an ordered mesostructures; and the silica prepared at pH 3.2 show a broad

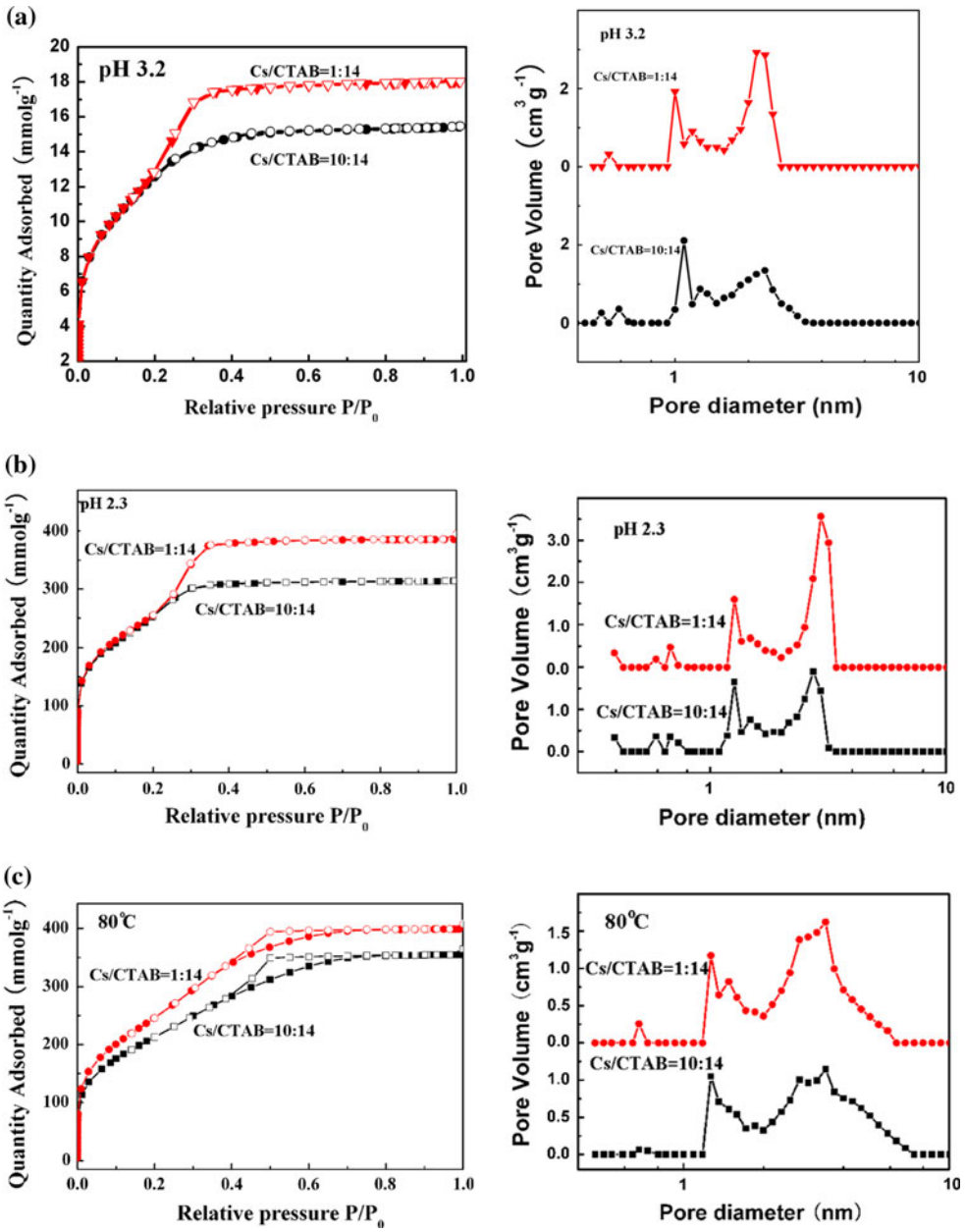

Fig. 7 N_2 adsorption–desorption isotherms and the pore size distribution of silica synthesized with the chitosan-CTAB hybrid via the sol-gel method at (**a**) pH 3.2 and (**b**) pH 2.3, or (**c**) via the hydrothermal method

Table 3 Structural parameters of micro–meso porous silica synthesized with the hybrid of chitosan (DD 59%)–CTAB

	Cs/CTAB	S_{BET} ($m^2\ g^{-1}$)	V_{total} ($cm^3\ g^{-1}$)	Microporosity (%)
Sol–gel	1:14	1069	0.625	51
pH = 3.2	10:14	1047	0.536	71
Sol–gel	1:14	929	0.611	57
pH = 2.3	10:14	925	0.486	71
Hydrothermal	1:14	911	0.630	47
pH = 3.2	10:14	787	0.564	47

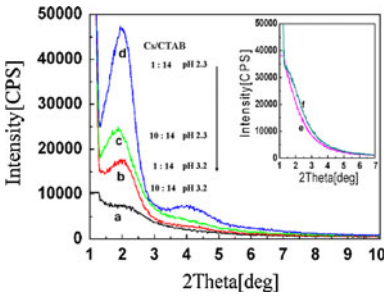

Fig. 8 XRD patterns of micro–meso porous silica synthesized with the chitosan–CTAB hybrid via the sol–gel method or the hydrothermal method (the *inset*), respectively

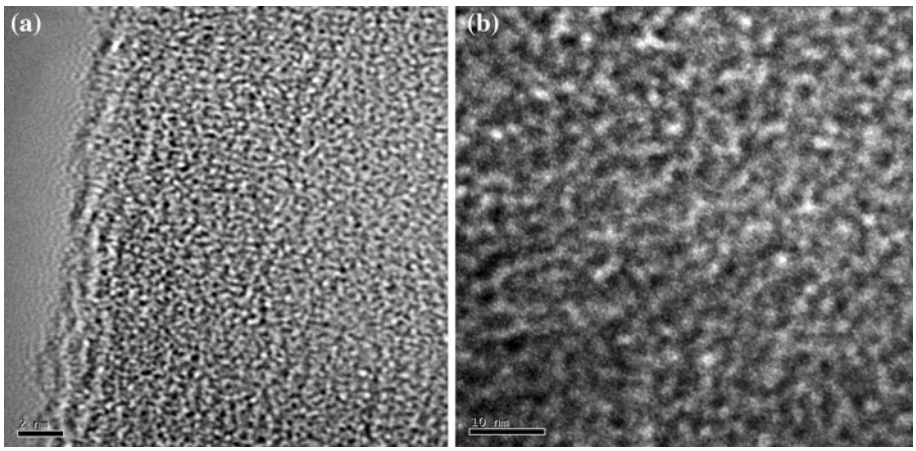

Fig. 9 TEM images of silica samples synthesized with the hybrid of CTAB and chitosan (**a** DD 88%, **b** DD 59%)

peak near 2.0° with low intensity. Whereas the silica synthesized via the hydrothermal method exhibit no peaks around 2.0°. Figure 9 illustrates clearly the orderly mesopores of silica samples synthesized via the sol–gel method at pH 2.3 with the hybrid of CTAB and chitosan (DD 88% and 59%).

The above reflection–absorption infrared spectra illustrates that the molecular orientations around the C=O groups and the NH_2 groups of chitosan are greatly affected by adding CTAB especially at lower pH, thus, the better meso-periodity of silica synthesized via the sol–gel at pH 2.3 is resulted from the inter-molecular interactions between chitosan and CTAB.

Conclusions

In this article, microporous silica samples were synthesized via the sol–gel method using the template of chitosan with the concentration near its CAC, which is related with the DD of chitosan. The interactions between chitosan and CTAB were studied by reflection–absorption infrared spectra, which illustrate that the molecular orientations around the C=O groups and the NH_2 groups of chitosan are greatly affected by adding CTAB especially at lower pH. CMC values of CTAB were measured using fluorescence probe techniques. The results indicate that there is a definite CMC of CTAB in the water–ethanol solvent at 30 °C and pH 6.1, whereas a relatively broad range of CTAB concentration exists at 30 °C and lower pH or at higher temperature corresponding to a slow transition process of micelles. Combining with characterizations of micro–meso porous silica synthesized with the chitosan–CTAB hybrid, it is illustrated that both the surface area and the pore volume as well as the meso-periodity of silica can be modulated by adding CTAB in the sol–gel synthesis process at proper pH value.

Acknowledgements The work described here is sponsored by the NSFC (no. 20576090, 20776102 and 20836005), RFDP20070056023, the Special Funds for Major State Basic Research Program of China (2006CB202500), the state key laboratory of catalytic material and research engineering (RIPP, SINOPEC), and the NCET. We greatly appreciate Professor Z. Conrad Zhang, Professor at the University of Texas, Austin, for his useful suggestions on this paper.

References

1. Agnihotri SA, Mallikarjuna NN, Aminabhavi TM (2004) J Controlled Release 100:5
2. Grenha A, Seijo B, Remuna López C (2005) Eur J Pharm Sci 25:427
3. Thongngam M, McClements DJ (2004) J Agric Food Chem 52:987
4. Thongngam M, McClements DJ (2005) Langmuir 21:79
5. Li Y, Xu G, Wu D, Sui W (2007) Eur Polym J 43:2690
6. Bao H, Li L, Zhang H (2008) J Colloid Interface Sci 328:270
7. Chiu JJ, Pine DJ, Bishop ST, Chmelka BF (2004) J Catal 221:400
8. Taguchi A, Schüth F (2005) Micropor Mesopor Mater 77:1
9. Zhang L, Qiao SZ, Jin YG, Yang HG, Budihartono S, Stahr F, Yan ZF, Wang XL, Hao ZP, Lu GQ (2008) Adv Funct Mater 18:3203
10. Zhao JW, Gao F, Fu YL, Jin W, Yang PY, Zhao DY (2002) Chem Commun 7:752
11. Zhang L, Qiao SZ, Jin YG, Cheng L, Yan ZF, Lu GQ (2008) Adv Funct Mater 18:3834
12. Zhu YF, Shi JL, Shen WH, Dong XP, Feng JW, Ruan ML, Li YS (2005) Angew Chem Int Ed 44:5083
13. Yang H, Zhu GS, Zhang DL, Xu D, Qiu SL (2007) Micropor Mesopor Mater 102:95
14. Pereira F, Valle K, Belleville P, Morin A, Lambert S, Sanchez C (2008) Chem Mater 20:1710
15. Ma XD, Sun HW, Yu P (2008) J Mater Sci 43:887. doi: 10.1007/s10853-007-2189-2
16. Lin CX, Yuan P, Yu CZ, Qiao SZ, Lu GQ (2009) Micropor Mesopor Mater 126:253
17. Yu CZ, Yu YH, Miao L, Zhao DY (2001) Micropor Mesopor Mater 44:65
18. Jang J, Bae J (2006) J Non-Cryst Solids 352:3979
19. Pang JB, Na H, Lu YF (2005) Micropor Mesopor Mater 86:89

20. Zou ZQ, Meng M, Zha YQ, Liu Y (2008) J Mater Sci 43:1958. doi:10.1007/s10853-008-2460-1
21. Pedroni V, Schulz PC, Ferreira MEGD, Morini MA (2000) Colloid Polym Sci 278:964
22. Pedroni VI, Schulz PC, Gschaider ME, Andreucetti N (2003) Colloid Polym Sci 282:100
23. Berth G, Dautzenberg H (2002) Carbohydr Polym 47:39
24. Li W, Han YC, Zhang JL, Wang BG (2005) Colloid J 67:159
25. Yang DJ, Li JP, Xu Y (2006) Micropor Mesopor Mater 95:180
26. Do DD, Nguyen C, Do HD (2001) Colloids Surf A 187–188:51
27. Esparza JM, Ojeda ML, Campero A, Hernandez G, Felipe C, Asomoza M, Cordero S, Kornhauser I, Rojas F (2005) J Mol Catal A 228:97
28. Zhang JM, Zhang DH, Shen DY (2002) Macromolecules 35:5140
29. Shen DY (1982) Applications of infrared spectrometer in polymers. Scientific Press, Beijing, p 48